Chem. Res. Chin. Univ., 2015, 31(5), 712—718 doi: 10.1007/s40242-015-5051-0

Synthesis, Structures and Properties of Three New Compounds Based on Multidentate Ligand Containing Triazole and Pyrimidine

LÜ Lei, MU Bao, LI Na and HUANG Rudan*

Key Laboratory of Cluster Science, Ministry of Education, Department of Chemistry, Beijing Institute of Technology, Beijing 100081, P. R. China

Abstract Three new compounds, namely, $[Zn(mtpo)_2(H_2O)_4]$(**1**), $[Cd(mtpo)_2{\cdot}CH_3CH_2OH]_n$(**2**) and $[Mn(mtpo)_2{\cdot}CH_3CH_2OH]_n$(**3**)(Hmtpo=4,7-dihydro-5-methyl-7-oxo-[1,2,4]triazolo[1,5-a]pyrimidine), have been synthesized *via* hydrothermal or solvothermal methods and characterized by means of elemental analyses, Fourier transform infrared(FTIR) spectroscopy, powder X-ray diffraction(PXRD), thermogravimetric analysis(TGA) and single-crystal X-ray diffraction. The results obtained from the single-crystal X-ray diffraction indicate that compound **1** has a mononuclear structure, and crystallizes in a monoclinic crystal system with $P2_1/c$ space group, which exhibits a 2D supramolecular network constructed by hydrogen bonds and π-π interactions. Compounds **2** and **3** are isomorphous and crystallize in a tetragonal system with space group of $I4_1/a$. The M^{2+}(M=Cd, Mn) ions in compounds **2** and **3** have the octahedral coordination geometry. Hmtpo acts as a bridging ligand linking the metal ions to form an infinite 3D framework with 4-connected $\{4^2{\cdot}8^4\}$ topology. There are hydrogen bonds between the guest ethanol molecules and the $mtpo^-$ ligands, which make the ethanol molecules exist in a 3D framework. In addition, luminescent properties of compounds **1** and **2** as well as magnetic property of compound **3** were investigated and water vapor adsorption and nitrogen sorption for compounds **2** and **3** were researched at 298 and 77 K, respectively.

Keywords Metal-organic framework(MOF); Hydrogen bond; Luminescent property; Magnetic property; Water vapor sorption; Nitrogen sorption

1 Introduction

Metal-organic frameworks(MOFs) have attracted great attention due to their intriguing variety of architectures and topologies, and their potential applications in the fields of gas storage, chemical separation, heterogeneous catalysis, as well as their potential utilization as optical, electronic and magnetic materials[1—8]. Organic ligands are one of the most important factors in the course of constructing MOFs. The ligands having one or several azole rings have a wide variety of coordination modes, such as monodentate, bidentate, tridentate and chelating, and can be used to construct novel topology structures and new functional materials[9—13]. 1,2,4-Triazolo[1,5-a]pyrimidine(tp) and its derivatives are very important ligands containing 1,2,4-triazole and pyrimidine rings, which possess abundant coordination nodes and strong coordination abilities[14,15]. As a multidentate bridging ligand, tp contains three nitrogen atoms, which can coordinate with metal ions to construct the intriguing multifarious structures exhibiting biological activity, luminescence and magnetism properties[16—23]. 4,7-Dihydro-5-methyl-7-oxo-[1,2,4] triazolo[1,5-a] pyrimidine(Hmtpo) is one of derivatives of 1,2,4-triazolo[1,5-a]pyrimidine(Scheme 1). The introduction of hydroxyl group substitute in the pyrimidine ring can afford more potential coordination modes and stronger coordination abilities. However, to our knowledge, only a few Hmtpo-based compounds have been reported[24—35]. Haasnoot and his co-workers[24] developed a Cu-Hmtpo mononuclear structure, which displayed significant magnetic interaction. Yao's group[33] reported the isostructural 3D *lvt* topology frameworks based on Co^{2+}, Ni^{2+} and versatile Hmtpo ligand. The rational design and construction of MOFs based on Hmtpo ligand are still worth further researching.

Herein, we synthesized three compounds, namely, $[Zn(mtpo)_2(H_2O)_4]$(**1**), $[Cd(mtpo)_2{\cdot}CH_3CH_2OH]_n$(**2**) and $[Mn(mtpo)_2{\cdot}CH_3CH_2OH]_n$(**3**), *via* hydrothermal or solvothermal methods. Compound **1** exhibits a 2D supramolecular network based on mononuclear structure, while compounds **2** and **3** are 3D frameworks with $\{4^2{\cdot}8^4\}$ Schläfli symbol. In the title compounds, the coordination modes of the Hmtpo ligand have an effect on the final skeleton. Furthermore, luminescent properties of compounds **1** and **2** as well as magnetic property of compound **3** were investigated and water vapor adsorption and nitrogen sorption for compounds **2** and **3** were also reported.

*Corresponding author. E-mail: huangrd@bit.edu.cn

Received February 9, 2015; accepted June 5, 2015.

Supported by the National Natural Science Foundation of China(Nos.21271024, 20971014) and the Natural Science Foundation of Beijing City, China(No.2112037).

© Jilin University, The Editorial Department of Chemical Research in Chinese Universities and Springer-Verlag GmbH

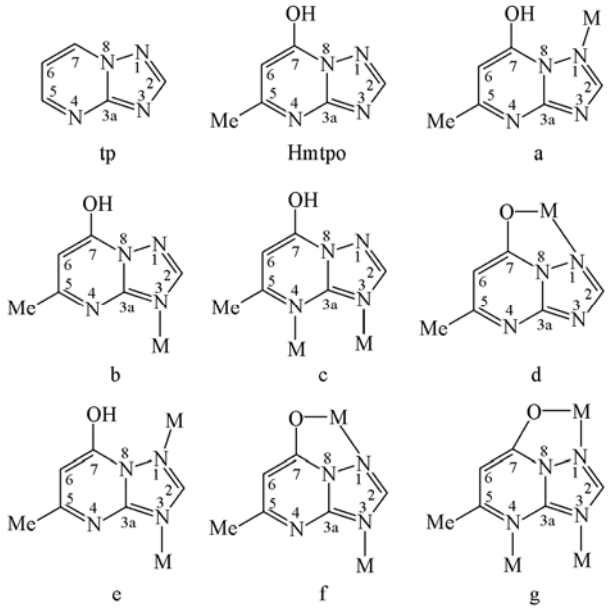

Scheme 1 Coordination modes of Hmtpo ligands

a. Monodentate; b. monodentate; c. bidentate; d. chelate; e. bidentate; f. chelate-monodentate; g. chelate-bidentate.

2 Experimental

2.1 Materials and Instruments

All the reagents and solvents were purchased from commercial sources and used without further purification. Elemental analyses(C, H and N) were performed on a Perkin-Elmer 2400 CHN element analyzer at room temperature. FTIR spectra were recorded in the 4000—400 cm^{-1} range on a Nicolet 170SX spectrophotometer with KBr pellets at room temperature. Powder X-ray diffraction(PXRD) data were collected on a Shimadzu XRD-6000 diffractometer with Cu *Kα* radiation. Thermogravimetric analysis(TGA) experiments were carried out on a Perkin-Elmer TGA 7 analyzer with a heating rate of 10 °C/min at temperatures from room temperature(r. t.) to 800 °C under the protection of nitrogen atmosphere. Luminescent spectra for the solid samples were measured on a Hitachi F-7000 FL spectrophotometer at room temperature. The photomultiplier detector voltage was 800 V and the instrument excitation and emission slits were set at 2.5 and 1.0 nm, respectively. The variable-temperature magnetic susceptibility measurements were carried out on a Quantum Design PPMS60000 in the temperature range of 1.8—300 K operating at 8.0×10^4 A/m. Water vapor adsorption studies were performed on a BELSORP MAX(BEL Japan) volumetric adsorption analyzer. Nitrogen adsorption experiments were conducted at 77 K on a TriStarII3020(Micromeritics Instrument Corporation) apparatus.

2.2 Synthesis of $[Zn(mtpo)_2(H_2O)_4]$(1)

A mixture of Hmtpo(0.0752 g, 0.5 mmol), $Zn(OAc)_2\cdot 2H_2O$(0.0550 g, 0.25 mmol) and distilled H_2O(8 mL) was sealed in a 23 mL Teflon-lined steel vessel and heated at 120 °C for 72 h. After the system was cooled to room temperature, colorless block crystals of compound **1** were obtained and washed with distilled water. The yield was *ca*. 35% based on Zn, and the yield of crystals was 0.0381 g. Elemental anal.(%) calcd. for $C_{12}H_{18}ZnN_8O_6$: C 33.08, H 4.16, N 25.72; found: C 33.17, H 4.11, N 25.73. IR(KBr), $\tilde{\nu}/cm^{-1}$: 3384(s), 1635(s), 1525(s), 1444(m), 1426(m), 1363(m), 1228(m), 1195(m), 1138(w), 983(w), 906(w), 840(w), 772(w).

2.3 Synthesis of $[Cd(mtpo)_2\cdot CH_3CH_2OH]_n$(2)

A mixture of Hmtpo(0.0752 g, 0.5 mmol), $Cd(OAc)_2\cdot 2H_2O$(0.0668 g, 0.25 mmol), an aqueous solution of 35%(mass fraction) Et_4NOH(0.04 mL) and CH_3CH_2OH(8 mL) was sealed in a 23 mL Teflon-lined steel vessel and heated at 120 °C for 72 h. After the system was cooled to room temperature, colorless block crystals of compound **2** were obtained and washed with ethanol. The yield was *ca*. 67% based on Cd, and the yield of crystals was 0.0765 g. Elemental anal.(%). calcd. for $C_{14}H_{16}CdN_8O_3$: C 36.82, H 3.53, N 24.53; found: C 36.84, H 3.55, N 24.48. IR(KBr), $\tilde{\nu}/cm^{-1}$: 3450(s), 1630(s), 1525(s), 1427(m), 1239(m), 1189(s), 1138(w), 1001(w), 813(w), 71(w).

2.4 Synthesis of $[Mn(mtpo)_2\cdot CH_3CH_2OH]_n$(3)

The synthesis of compound **3** was similar to that of compound **2**, except that $Mn(OAc)_2\cdot 4H_2O$(0.0620 g, 0.25 mmol) was used instead of $Cd(OAc)_2\cdot 2H_2O$ and the temperature of the reaction mixture was 150 °C. After the system was cooled to room temperature, red block crystals of compound **3** were obtained and washed with ethanol. The yield was *ca*. 39% based on Mn, and the yield of crystals is 0.0389 g. Elemental anal.(%) calcd. for $C_{14}H_{16}MnN_8O_3$: C 42.11, H 4.04, N 28.06; found: C 42.18, H 3.99, N 28.12. IR(KBr), $\tilde{\nu}/cm^{-1}$: 3446(s), 1636(s), 1529(s), 1440(m), 1187(w), 1138(w), 998(w), 813(m), 773(m).

2.5 X-Ray Crystallography

Single-crystal X-ray diffraction data for compounds **1—3** were collected on a Bruker Smart-1000 CCD diffractometer equipped with a graphite-monochromatized Mo *Kα* radiation (λ=0.071073 nm). The intensity data were collected at 293 K and the structures were solved by direct methods and expanded using Fourier techniques with SHELXL-97 program[36]. The non-hydrogen atoms were refined anisotropically by full-matrix least-squares calculations on F^2. The hydrogen atoms were added theoretically, riding on the concerned atoms and were not refined. In compounds **2** and **3**, the carbon atoms and oxygen atoms of the guest molecules CH_3CH_2OH were split in two sites(each had half-occupancy). A summary of crystallographic data and structure refinements for compounds **1—3** is given in Table 1. Selected bond lengths and bond angles for compounds **1—3** are listed in Tables S1—S3 (see the Electronic Supplementary Material of this paper). Hydrogen bonding geometries are summarized in Tables S4—S6(see the Electronic Supplementary Material of this paper). CCDC reference numbers of 974838—974840 contain the supplementary crystallographic data for compounds **1—3**. These data can be obtained free of charge from the Cambridge

Table 1 Crystal data and structure refinement summary for compounds 1—3

Compound	**1**	**2**	**3**
Empirical formula	$C_{12}H_{18}N_8O_6Zn$	$C_{14}H_{16}N_8O_3Cd$	$C_{14}H_{16}N_8O_3Mn$
Formula weight	435.73	456.76	399.29
Crystal system	Monoclinic	Tetragonal	Tetragonal
Space group	$P2_1/c$	$I4_1/a$	$I4_1/a$
a/nm	0.91523(8)	1.73655(15)	1.71232(4)
b/nm	1.39560(9)	1.73655(15)	1.71232(4)
c/nm	0.68513(5)	1.15508(9)	1.13086(5)
α/(°)	90	90	90
β/(°)	108.602(2)	90	90
γ/(°)	90	90	90
V/nm^3	0.82939(11)	3.48330(5)	3.31573(18)
Z	2	8	8
D_c/(Mg·m^{-3})	1.745	1.742	1.600
T/K	293(2)	293(2)	293(2)
μ/mm^{-1}	1.534	1.287	0.831
F(000)	448	1824	1640
θ range/(°)	2.76—25.02	3.16—25.01	3.21—25.00
Reflection collected/unique	4601/1464	8578/1538	2935/1460
R_{int}	0.0547	0.0320	0.0406
Datum/restrain/ parameter	1464/0/125	1538/2/135	1460/0/134
GOF on F^2	1.077	1.180	1.052
$R_1{}^a/wR_2{}^b[I>2\sigma(I)]$	0.0434/0.1121	0.0247/0.0558	0.0485/0.1080
R_1/wR_2(all reflect.)	0.0515/0.1203	0.0335/0.0649	0.0668/0.1248

a. $R_1=\sum||F_o|-|F_c||/\sum|F_o|$; *b*. $wR_2=[\sum w(F_o^2-F_c^2)^2/\sum w(F_o^2)^2]^{1/2}$.

Crystallographic Data Centre *via* http://www.ccdc.cam.ac.uk/data_request/cif.

3 Results and Discussion

3.1 Synthesis and Crystal Structure

As shown in Scheme 2, compounds **1—3** were prepared under hydrothermal or solvothermal reaction conditions. Although the same molar ratio of Hmtpo ligand to metal ion(2:1) was adopted, the structure of compound **1** is different from those of compounds **2** and **3**. Compound **1** was obtained in the absence of the Et_4NOH, which might play a significant role in the formation of mononuclear compound. Compounds **2** and **3** are 3D MOFs. Though the reaction temperatures for compound **2**(120 °C) and compound **3**(150 °C) are different, they are isomorphous. This may suggest that the reaction temperature do not affect the structures of compounds **2** and **3**.

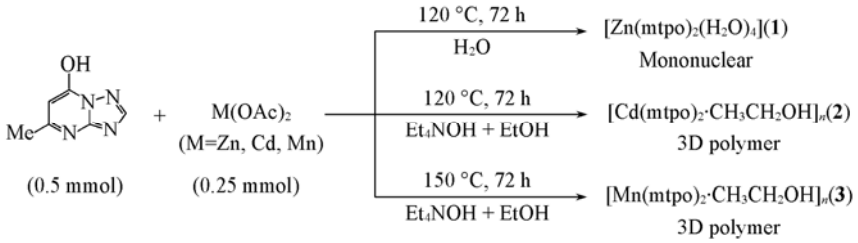

Scheme 2 Synthetic routes of compounds 1—3

Single-crystal X-ray diffraction analysis reveals that compound **1** crystallizes in a monoclinic crystal system with $P2_1/c$ space group, and there are one Zn^{2+} ion, one $mtpo^-$ ligand and two coordinated water molecules in the asymmetric unit. The Zn^{2+} ion is six coordinated with two nitrogen atoms(N3, N3A) from two $mtpo^-$ ligands and four oxygen atoms(O2, O2A, O3, O3A) from four coordinated water molecules to form a slightly distorted octahedral geometry(Fig.1). The $mtpo^-$ ligand acting as a monodentate ligand employs the N atom at position 3(Scheme 1 mode b). In the arrangement of the distorted octahedral coordination geometry, N3 and N3A atoms occupy the axial positions, and O2, O2A, O3 and O3A atoms reside in the equatorial positions. The bond distances of Zn1—N3, Zn1—O2 and Zn1—O3 are 0.2054(3), 0.2148(2) and 0.2189(2) nm, respectively, which are within the normal range[23]. The bond angle of N3—Zn1—N3A is 180.0°, while those of N3—Zn1—O_{aqua} vary from 88.13° to 91.87°. The bond angles between Zn1 and the coordinated water molecules vary from 85.14° to 180.00°(Table S1).

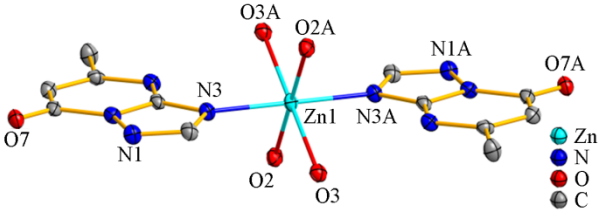

Fig.1 Coordination environment of Zn^{2+} ion in compound 1

Hydrogen atoms are omitted for clarity. Symmetry code: A. $-x+1, -y+1, -z$.

It is noteworthy that there are various hydrogen bonds and π-π interactions between the adjacent $[Zn(mtpo)_2(H_2O)_4]$ molecules. As shown in Fig.S1(see the Electronic Supplementary Material of this paper), four coordinated water molecules from one $[Zn(mtpo)_2(H_2O)_4]$ molecule act as bridges to connect four adjacent $[Zn(mtpo)_2(H_2O)_4]$ molecules *via* intermolecular hydrogen bonds{O2−H2B···O7[0.2819(4) nm], O2−H2C···N1 [0.2927(4) nm] and O3−H3C···O7[0.2755(4) nm]} to generate a 2D supramolecular network in the *bc* plane. It is interesting to note that this 2D supramolecular network also can be obtained *via* π-π interactions. The centroid-centroid distances of two stacking pyrimidine rings and two stacking triazole rings are 0.3437(18) and 0.3492(19) nm, respectively, which are within the normal range(0.33—0.38 nm)[37]. Hydrogen bonds and π-π interactions have an effect on the consolidation of the 2D supramolecular network(Fig.2).

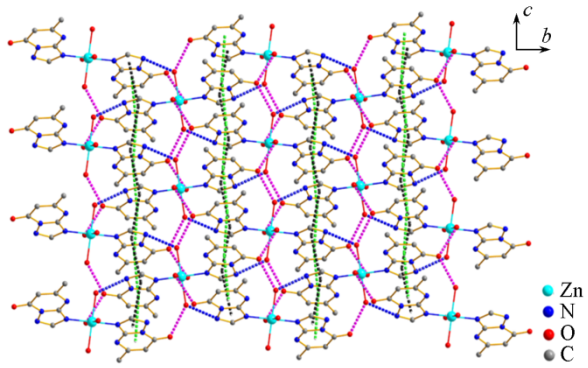

Fig.2 2D supramolecular network of compound 1 constructed by hydrogen bonds and π-π interactions in the *bc* plane

Hydrogen atoms are omitted for clarity.

Single-crystal X-ray diffraction analyses reveal that compounds **2** and **3** are isomorphous and crystallize in a tetragonal system with space group of $I4_1/a$. Herein, we discussed compound **3** in detail as an example. The asymmetric unit of compound **3** contains one Mn^{2+} ion, one half-occupied and two quarter-occupied $mtpo^-$ ligands, and one guest ethanol molecule. As shown in Fig.3, the crystallographically independent Mn^{2+} ion is six-coordinated by two hydroxyl oxygen atoms(O7 and O7A) and four nitrogen atoms(N1, N1A, N3 and N3A)

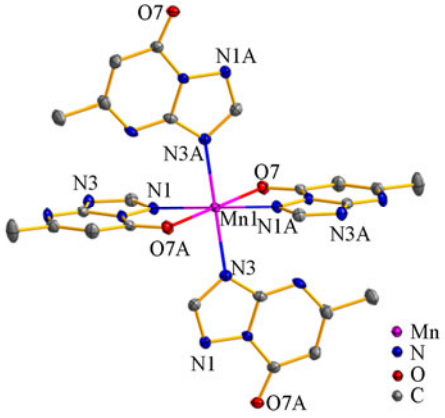

Fig.3 Coordination environment of Mn^{2+} ion in compound 3

Hydrogen atoms and guest CH_3CH_2OH molecules are omitted for clarity. Symmetry code: A. $-x+2, -y+1, -z+2$.

from four $mtpo^-$ ligands in a slightly distorted octahedral geometry. Two $mtpo^-$ ligands act as monodentate N-donor ligand, while the other two $mtpo^-$ ligands act as bidentate chelating ligand, the N1 and O7 atoms of which coordinate to Mn^{2+} ion, forming two stable five-membered chelate rings. The bond lengths of Mn1—N1, Mn1—N3 and Mn1—O7 are 0.2282(3), 0.2250(3) and 0.2198(2) nm, respectively, which are typical distances of Mn—N and Mn—O bonds[38]. The bond angles of N3—Mn1—N1, N3—Mn1—O7 and N3—Mn1—N3A are 89.89°, 91.69° and 180.0°, respectively, while those of N1—Mn1—O7A, N1—Mn1—N1A and O7—Mn1—O7A are 75.30°, 180.0° and 180.0°, respecttively(Table S3).

The nitrogen atoms(N1 and N3) from triazole serveing as bridging linkers connect the adjacent Mn^{2+} ions to form a 3D open framework structure with the adjacent Mn···Mn distance being 0.6682(2) nm. In the 3D framework, there is a 1D right-handed helical channel along *c* axis with a window size of 0.679 nm×0.679 nm, and disordered ethanol molecules residing in it(Fig.4). Moreover, the ratio of the solvent-accessible void volume to the total crystal volume is about 21% for compound **3**(21.8% for compound **2**). As shown in Fig.S2(see the Electronic Supplementary Material of this paper), there exist hydrogen-bonding interactions between ethanol molecules(O1) and the $mtpo^-$ ligands(C8, O7) with distances of 0.2867(11) nm(O1···O7) and 0.3171(12) nm(C8···O1), respectively, which are shorter than those of the reported O···O bond(0.3115 nm)[39] and C···O bond(0.3479 nm)[7](Table S6). From the topological viewpoint, the $mtpo^-$ ligands can be regarded as a linker, while the Mn^{2+} ions can be regarded as 4-connected nodes linked by four $mtpo^-$ ligands to form a 4-connected 3D framework with construction of $\{4^2{\cdot}8^4\}$ Schläfli symbol(Fig.5).

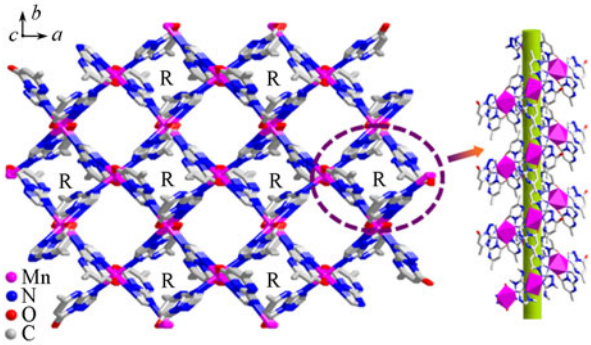

Fig.4 3D framework of compound 3(left) with a 1D right-handed helical channel along the *c* axis(right)

Hydrogen atoms and guest molecules CH_3CH_2OH are omitted for clarity.

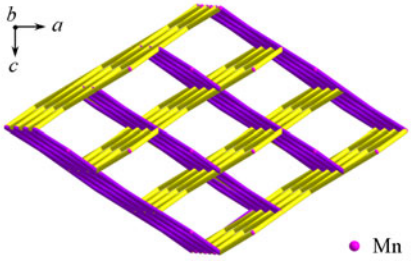

Fig.5 Topological structure of compound 3

3.2 Effect of Coordination Modes of Hmtpo Ligand on the Architectures of Compounds 1—3

Three new compounds **1—3** based on the same Hmtpo ligand and three kinds of metal ions were synthesized under the hydrothermal or solvothermal conditions. The Hmtpo ligand displays different coordination modes in the compounds **1—3**. For compound **1**, only one nitrogen atom(N3) from the mtpo$^-$ ligand coordinates with the Zn^{2+} ions to build a mononuclear structure, which is further extended into a 2D supramolecular network *via* hydrogen bonds and π-π interactions. While for compounds **2** and **3**, not only two nitrogen atoms(N1 and N3) from triazole but also one oxygen atom(O7) from hydroxyl group of the mtpo$^-$ ligand connects with the metal ions to form a 3D framework with $\{4^2\cdot8^4\}$ topology. It may be implied that the coordination modes of the ligand play a key role in the formation of the final architectures.

3.3 IR Spectra

The infrared spectra of compounds **1—3** are quite similar to each other. The strong and broad peaks at 3384, 3450 and 3446 cm^{-1} are ascribed to ν(OH) of the coordinated water molecules for compound **1** and guest ethanol molecules for compounds **2** and **3**, respectively. The free Hmtpo ligand has a broad maximum peak at 1700 cm^{-1}, which is ascribed to the C═O stretching vibration[40]. The absorption peaks shift to 1635, 1630 and 1636 cm^{-1} for compounds **1—3**, respectively, owing to the deprotonation of Hmtpo and the coordination of oxygen atoms to the metal ions[29,35].

3.4 PXRD Measurements

To confirm the phase purity and the crystallinity of the samples, powder X-ray diffraction analyses were carried out at room temperature. As shown in Fig.S3(see the Electronic Supplementary Material of this paper), the experimental patterns of compounds **1—3** are well consistent with the simulated ones which are derived from the single-crystal X-ray diffraction data. It can be confirmed that these samples have good phase purity and crystallinity.

3.5 Thermal Analysis

The thermal behaviors of compounds **1—3** were studied by TGA to estimate their thermal stabilities(Fig.6). For compound **1**, the first mass loss occurs at temperatures from 80 °C to 130 °C. The observed mass loss of 16.22% is in agreement with the calculated value(16.54%), and can be attributed to the loss of coordination water molecules. The anhydrous sample remains stable up to 340 °C and then the framework abruptly collapses. The TGA curve of compound **2** shows a gradual mass loss of 9.98%(calcd. 10.08%) from room temperature to 300 °C, which corresponds to the removal of guest ethanol molecules. The framework continues to decompose at 340 °C. The TGA curve of compound **3** shows a mass loss of 10.85%(calcd. 11.53%) in a temperature range from room temperature to 330 °C, which corresponds to the loss of lattice ethanol molecules. The decomposition of compound **3** continues at above 360 °C.

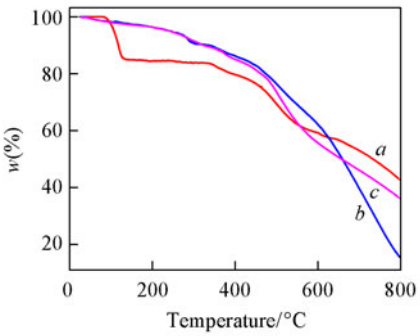

Fig.6 TGA curves for compounds 1—3(*a*—*c*)

3.6 Luminescence Properties

Compounds with d^{10} configuration metal centers have been investigated due to their potential utilizations as luminescent materials. The solid state luminescence spectra of Hmtpo, and compounds **1** and **2** were studied at room temperature under the same conditions. As shown in Fig.7, the Hmtpo ligand shows a fluorescent emission at 344 nm when excited at 314 nm. When excited at 318 nm(for compound **1**) and 281 nm(for compound **2**), the intense emission bands at 340 nm for compound **1** and 341 nm for compound **2** can be observed. The enhancement of luminescence intensity of compounds **1** and **2** may be attributed to the ligand chelation to the metal center, which effectively increases the rigidity of the ligand and reduces the loss of energy *via* radiationless decay[41,42]. Compared with the emission spectrum of the Hmtpo ligand, there is no significant change in the position of the maximum emission of compounds **1** and **2**, which can be attributed to ligand-ligand charge transfer(LLCT)[23,43].

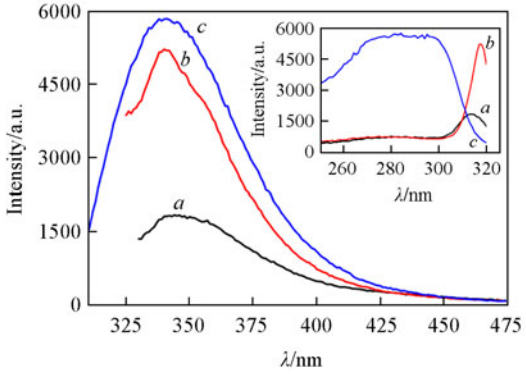

Fig.7 Solid state excitation(inset) and emission spectra of Hmtpo(*a*), and compounds 1(*b*) and 2(*c*) at room temperature

3.7 Magnetic Property

Variable-temperature magnetic susceptibility data of pure crystal sample were collected in the temperature range of 1.8—300 K. Plots of χ_M^{-1} *versus* T and $\chi_M T$ *versus* T of compound **3** are shown in Fig.8 to display the magnetic behavior. The isothermal field-dependent magnetizations $M(H)$ of compound **3** were measured at 1.8 K and fields up to 7 T(Fig.S4, see the Electronic Supplementary Material of this paper).

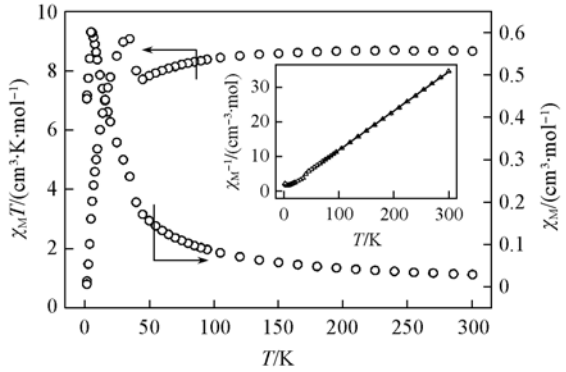

Fig.8 Plots of $\chi_M T$ *versus* T and χ_M *versus* T for compound 3

Inset: χ_M^{-1} *versus* T plot for compound 3(the straight line represents the best fit of the data based on the Curie-Weiss law).

The plot of χ_M^{-1} *versus* T of compound **3** displays Curie-Weiss behavior from 300 K to 70 K, and the best linear fit of $\chi_M^{-1}(T)$ data above 70 K results in C=8.86 cm^3·K·mol^{-1} and θ = –5.33 K. This negative Weiss constant indicates the presence of a very weak antiferromagnetic interaction between the spin centers. The $\chi_M T$ value of compound **3** at 300 K is 8.66 cm^3·K·mol^{-1}, which is close to the expected spin-only value for two isolated Mn^{2+} ion(S=5/2; g=2.00). The value of $\chi_M T$ remains almost constant as the temperature decreases to 120 K, then a slow decrease to a minimum of 7.71 cm^3·K·mol^{-1} at 45 K has been achieved. And then the value of $\chi_M T$ increases up to 9.12 cm^3·K·mol^{-1} at 35 K and finally drops sharply upon further cooling. It can be seen from the crystal structure of compound **3** that the 2D architecture is formed *via* linking the rectangle tetra-Mn(II) fragments with each other. And thus the antiferromagnetic coupling interactions may lead to a canting between the spins of Mn(II) at low temperatures. The magnetic behavior below 45 K may be resulted from the spin-canting in view of the crystal architecture, which is possible to present a 2D array of spins.

The maximum value of magnetization curve of compound **3** presented in Fig.S4 is far from the saturated one, further confirming the presence of dominant antiferromagnetic interaction. Also, the magnetization curve is nearly linear, indicating a paramagnetic state at a temperature of 1.8 K[44,45].

3.8 Water Vapor Sorption and Nitrogen Sorption of Compounds 2 and 3

The adsorption of water vapor by MOFs featuring good hydrothermal stability plays an important role in the capture and release of water[46,47]. To investigate the properties of water vapor adsorption of compounds **2** and **3**, the adsorption isotherms were obtained at 298 K. Before the measurements, the samples of compounds **2** and **3** were heated at 110 °C for 12 h under vacuum to remove the guest ethanol molecules of the 3D framework. As shown in Fig.9, the amount of water sorption increases sharply when p/p_0>0.4 and reaches 4.17 and 67.75 mL/g for compounds **2** and **3** at p/p_0=0.95, respectively. The desorption isotherms display the obvious hysteresis, illustrating that part of water molecules are adsorbed into the spaces of the 3D framework, which may be attributed to the hydrogen bonding interactions[48]. The PXRD patterns after activation and adsorption experiments, respectively, reveal the stability of the frameworks[Fig.S3(B) and (C)].

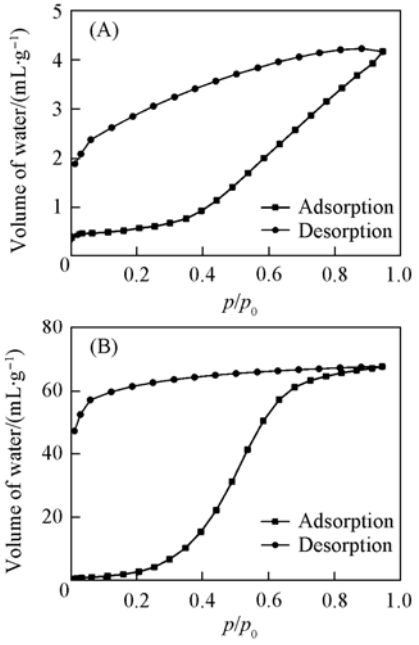

Fig.9 Water adsorption-desorption isotherms for compounds 2(A) and 3(B) at 298 K

To research the permanent porosity of compounds **2** and **3**, the N_2 sorption isotherms were performed at 77 K. N_2 sorption experiments were carried out upon heating at 110 °C under vacuum for 12 h to remove the guest ethanol molecules. As shown in Fig.S5(see the Electronic Supplementary Material of this paper), compounds **2** and **3** show type-II adsorption behaviours, and the uptake values of N_2 at 77 K are 18.8 cm^3/g for compound **2** and 60.5 cm^3/g for compound **3**. The related Brunauer-Emmett-Teller(BET) surface areas are 25.8 m^2/g for compound **2** and 86.2 m^2/g for compound **3**. The PXRD patterns after N_2 adsorption demonstrate that the frameworks retain the stability[Fig.S3(B) and (C)].

The above results show that although compounds **2** and **3** are isomorphous, there are great differences in the amount of water sorption or N_2 sorption for them. The results may be due to the difference of interaction between the metal ions and the gas molecules.

4 Conclusions

In summary, one mononuclear compound[$Zn(mtpo)_2(H_2O)_4$] (**1**) and two isomorphous polymeric compounds [$Cd(mtpo)_2{\cdot}CH_3CH_2OH]_n$(**2**) and [$Mn(mtpo)_2{\cdot}CH_3CH_2OH]_n$(**3**) were prepared by the reaction of 4,7-dihydro-5-methyl-7-oxo-[1,2,4]triazolo[1,5-a]pyrimidine(Hmtpo) ligand with the transition metal salts under hydrothermal or solvothermal conditions. Compound **1** exhibits a mononuclear structure, upon which a 2D supramolecular network can be formed *via* hydrogen bonds and π-π interactions. While compounds **2** and **3** display infinite 3D frameworks with the $\{4^2{\cdot}8^4\}$ topology. The luminescent property analyses show that compounds **1** and **2** may be the candidates for potential photoactive materials.

Magnetic property of compound **3** indicates that there is a very weak antiferromagnetic coupling interaction between Mn^{2+} ions. The properties of water vapor adsorption and nitrogen adsorption prove that compound **3** possesses good adsorption ability.

Electronic Supplementary Material

Supplementary material is available in the online version of this article at http://dx.doi.org/10.1007/S40242-015-5051-0.

References

[1] Suh M. P., Park H. J., Prasad T. K., Lim D. W., *Chem. Rev.*, **2012**, *112*(2), 782

[2] Li J. R., Sculley J., Zhou H. C., *Chem. Rev.*, **2012**, *112*(2), 869

[3] Yoon M., Srirambalaji R., Kim K., *Chem. Rev.*, **2012**, *112*(2), 1196

[4] Cui Y. J., Yue Y. F., Qian G. D., Chen B. L., *Chem. Rev.*, **2012**, *112*(2), 1126

[5] Wong-Foy A. G., Matzger A. J., Yaghi O. M., *J. Am. Chem. Soc.*, **2006**, *128*(11), 3494

[6] Wan Y., Zhang L., Jin L., Gao S., Lu S., *Inorg. Chem.*, **2003**, *42*(16), 4985

[7] Dong L. J., Chu W., Zhu Q. L., Huang R. D., *Cryst. Growth Des.*, **2011**, *11*(1), 93

[8] Zhao D., Timmons D. J., Yuan D. Q., Zhou H. C., *Acc. Chem. Res.*, **2011**, *44*(2), 123

[9] Zhang Z. Q., Huang R. D., Dong L. J., Xu Y. Q., Yu L. Q., Jiao Z. W., Hu C. W., *Inorg. Chim. Acta*, **2009**, *362*(9), 3056

[10] Dong L. J., Huang R. D., Wei Y. G., Chu W., *Inorg. Chem.*, **2009**, *48*(16), 7528

[11] Zhu Q. L., Huang R. D., Lu K., Dong L. J., Hu C. W., *Inorg. Chim. Acta*, **2009**, *362*(14), 4943

[12] Wang B., Furukawa H., Yaghi O. M., *Nature*, **2008**, *453*, 207

[13] Hayashi H., Furukawa H., Yaghi O. M., *Nat. Mater.*, **2007**, *6*, 501

[14] Salas J. M., Romero M. A., Sánchez M. P., Quirós M., *Coord. Chem. Rev.*, **2000**, *193—195*, 1119

[15] Haasnoot J. G., *Coord. Chem. Rev.*, **2000**, *200—202*, 131

[16] van Albada G. A., de Graaff R. A. G., Haasnoot J. G., Schild J., Reedijk J., *Acta Crystallogr., Sect. C: Cryst. Struct. Commun.*, **1991**, *47*, 943

[17] Maldonado C. R., Quirós M., Salas J. M., *Polyhedron*, **2008**, *27*(13), 2779

[18] Machura B., Jaworska M., Lodowski P., Kusz J., Kruszynski R., Mazurak Z., *Polyhedron*, **2009**, *28*(13), 2571

[19] Navarro J. A. R., Salas J. M., Romero M. A., Faure R., *J. Chem. Soc., Dalton Trans.*, **1998**, 901

[20] Caballero A. B., Rodríguez-Diéguez A., Vieth J. K., Salas J. M., Janiak C., *Inorg. Chim. Acta*, **2011**, *376*(1), 674

[21] Caballero A. B., Vieth J. K., Rodríguez-Diéguez A., Vidal I., Salas J. M., Janiak C., *Dalton Trans.*, **2011**, (40), 11845

[22] Caballero A. B., Marín C., Rodríguez-Diéguez A., Quirós M., Salas J. M., Sánchez-Moreno M., *Polyhedron*, **2012**, *33*(1), 137

[23] Caballero A. B., Rodríguez-Diéguez A., Barea E., Quirós M., Salas J. M., *Cryst. Eng. Comm.*, **2010**, (12), 3038

[24] Dirks E. J., Haasnoot J. G., Kinneging A. J., Reedijk J., *Inorg. Chem.*, **1987**, *26*(12), 1902

[25] Salas J. M., Navarro J. A. R., Romero M. A., Quirós M., *An. Quim. Int. Ed.*, **1997**, *93*, S49

[26] Navarro J. A. R., Romero M. A., Salas J. M., Quirós M., Tiekink E. R. T., *Inorg. Chem.*, **1997**, *36*(22), 4988

[27] Navarro J. A. R., Romero M. A., Salas J. M., Quirós M., *Inorg. Chem.*, **1997**, *36*(15), 3277

[28] Navarro J. A. R., Salas J. M., Romero M. A., Vilaplana R., Gonzalez-Vílchez F., Faure R., *J. Med. Chem.*, **1998**, *41*(3), 332

[29] Navarro J. A. R., Romero M. A., Salas J. M., Molina J., Tiekink E. R. T., *Inorg. Chim. Acta*, **1998**, *274*(1), 53

[30] Lakomska I., Wojtczak A., Sitkowski J., Kozerski L., Szlyk E., *Polyhedron*, **2007**, *26*(4), 803

[31] Navarro J. A. R., Romero M. A., Salas J. M., Quirós M., Molina J., *Inorg. Chem.*, **1996**, *35*(26), 7829

[32] Navarro J. A. R., Romero M. A., Salas J. M., *J. Chem. Soc., Dalton Trans.*, **1997**, 1001

[33] Lin Q. P., Zhang J., Cao X. Y., Yao Y. G., Li Z. J., Zhang L., Zhou Z. F., *Cryst. Eng. Comm.*, **2010**, (12), 2938

[34] Navarro J. A. R., Romero M. A., Salas J. M., Faure R., Solans X., *J. Chem. Soc., Dalton Trans.*, **1997**, 2321

[35] Han Z. P., Li Y. H., *Inorg. Chem. Commun.*, **2012**, *22*, 73

[36] Sheldrick G. M., *SHELXL-97 and SHELXS-97*, *Program for Crystal Structure Solution*, University of Göttingen, Göttingen, **1997**

[37] Janiak C., *J. Chem. Soc. Dalton Trans.*, **2000**, 3885

[38] Briceno A., Leal D., Atencio R., de Delgado G. D., *Chem. Commun.*, **2006**, 3534

[39] Liu Z., Chen Y., Liu P., Wang J., Huang M. H., *J. Solid State Chem.*, **2005**, *178*(7), 2306

[40] Becket A. H., Spickett R. G. W., Wright S. H. B., *Tetrahedron*, **1968**, *24*(7), 2839

[41] Zheng S. L., Tong M. L., Tan S. D., Wang Y., Shi J. X., Tong Y. X., Lee H. K., Chen X. M., *Organometallics,* **2001**, *20*(25), 5319

[42] Cao X. Y., Li Z. J., Zhang J., Qin Y. Y., Cheng J. K., Yao Y. G., *Cryst. Eng. Comm.*, **2008**, (10), 1345

[43] Wang X. S., Tang Y. Z., Huang X. F., Qu Z. R., Che C. M., Xiong R. G., *Inorg. Chem.*, **2005**, *44*(15), 5278

[44] Earl L. D., Patrick B. O., Wolf M. O., *Inorg. Chem.*, **2013**, *52*(17), 10021

[45] Chen X., Wang Y. Y., Liu B., Yin B., Liu P., Shi Q. Z., *Dalton Trans.*, **2013**, (42), 7092

[46] Čelič T. B., Mazaj M., Guillou N., Elkaïm E., Roz M. E., Thibault-Starzyk F., Mali G., Rangus M., Čendak T., Kaučič V., Logar N. Z., *J. Phys. Chem. C*, **2013**, *117*(28), 14608

[47] Furukawa H., Gándara F., Zhang Y. B., Jiang J. C., Queen W. L., Hudson M. R., Yaghi O. M., *J. Am. Chem. Soc.*, **2014**, *136*(11), 4369

[48] Cao X. Y., Mu B., Huang R. D., *Cryst. Eng. Comm.*, **2014**, (16), 5093